Experimental and Molecular Pathology 111 (2019) 104301

Contents lists available at ScienceDirect

Experimental and Molecular Pathology

journal homepage: www.elsevier.com/locate/yexmp

# Hypoxia induced microRNA-301b-3p overexpression promotes proliferation, migration and invasion of prostate cancer cells by targeting LRP1B

Haiying Zheng[a], Ligang Bai[b,*]

[a] Department of Cardiovascular Medicine, The Affiliated Hospital of Inner Mongolia Medical University, Huhhot 010050, PR China
[b] Department of Urology Surgery, The Affiliated Hospital of Inner Mongolia Medical University, Huhhot 010050, PR China

ARTICLE INFO

*Keywords:*
Hypoxia
microRNA-301b-3p
LRP1B
Prostate cancer
Proliferation
Migration
Invasion

ABSTRACT

Prostate cancer is a high burden on society worldwide due to its high morbidity and mortality. Growing evidence has implicated microRNAs (miRNAs or miRs) in the occurrence and progression of prostate cancer. The present study was conducted with main emphasis put on the possible effect of hypoxia-induced miR-301b-3p on prostate cancer by targeting low-density lipoprotein receptor-related protein 1B (LRP1B). Firstly, the differentially expressed genes were identified by conducting microarray-based gene expression profiling of prostate cancer. Next, the expression of miR-301b-3p in prostate cancer cells was examined in cells treated with 1% oxygen or dimethyloxalylglycine (DMOG), and the cell line with the highest miR-301b-3p expression was selected for subsequent experiments. Subsequently, the target relationship between miR-301b-3p and LRP1B was identified. The effect of miR-301b-3p and LRP1B on cell proliferation, migration and invasion as well as tumorigenicity of transfected cells was examined using the gain- and loss-of-function approaches. Hypoxia induced miR-301b-3p was highly expressed while LRP1B was poorly expressed in prostate cancer. Moreover, miR-301b-3p could down-regulate LRP1B by interacting with LRP1B, which acted to promote the proliferation, migration and invasion abilities of prostate cancer cells in addition to tumor growth in vivo. In addition, up-regulation of LRP1B can reverse the promoting effect of miR-301b-3p on the aforementioned factors. Collectively, up-regulation of miR-301b-3p induced by hypoxia could potentially accelerate proliferation, migration and invasion of prostate cancer cells via the inhibitory effect on LRP1B expression, highlighting that miR-301b-3p may be instrumental for the therapeutic targeting of prostate cancer.

## 1. Introduction

Prostate cancer represents the most frequently occurring non-cutaneous cancer accompanied by the highest morbidity and the second highest mortality among males (von Eyben et al., 2018). According to a previous study, there was little change in the mortality rates of prostate cancer in a period of 25 years from 1989 to 2014 (Chen et al., 2014). Due to the high mortality, prostate cancer remains to be one of the most serious burdens in health care (Huang et al., 2018). The challenges faced in the study of prostate cancer are also partially due to the involvement of large-scale multicenter genomics projects; therefore, the dissection of prostate tumor requires careful guidance from pathologists for its relatively smaller tumor size and the specialty of admixing with stroma (Taylor et al., 2010). Radiation therapy remains to be the main treatment option for localized prostate cancer, but radio-resistance of cancer cells makes recurrence a common event following treatment (Chang et al., 2014). Therefore, there's an urgent need to come up with novel diagnostic and prognostic biomarkers for prostate cancer that can distinguish mild and aggressive forms of prostate cancer, and thereby aid the management and provide more effective therapeutic options (Fort et al., 2018).

Low-density lipoprotein receptor-related protein 1B (LRP1B) forms a member of the low-density lipoprotein receptor gene family, which is a group of membrane receptors that have been the center of multiple researches in recent years, as they play multiple roles in cell signaling, developmental processes, and lipoprotein trafficking (Dietrich et al., 2010). LRP1B is one of the ten most largely missed genes in 3312 specimens of human cancer (Prazeres et al., 2011). The poor expression of LRP1B has been found in several primary cancers, making it a potential tumor suppressor (Ni et al., 2013; Wang et al., 2017). In the

* Corresponding author at: Department of Urology Surgery, The Affiliated Hospital of Inner Mongolia Medical University, No. 1, Tongdao North Road, Huimin District, Huhhot 010050, Inner Mongolia Autonomous Region, PR China.
*E-mail address:* doctor0778@sina.com (L. Bai).

https://doi.org/10.1016/j.yexmp.2019.104301
Received 23 April 2019; Received in revised form 19 July 2019; Accepted 20 August 2019
Available online 21 August 2019

present study, the results from the Targetscan website and dual luciferase reporter gene assay revealed that there is a specific binding region between LRP1B gene sequence and microRNA-301b-3p (miR-301b-3p) sequence. LRP1B was also identified as the target gene of miR-301b-3p. MicroRNAs (miRNAs or miRs) are small non-coding RNAs that have been found to play crucial roles in multiple biological processes, including host defense, cell development and proliferation (Li et al., 2016; Xiang et al., 2018). The miR-130 gene family is composed of miR-301b, along with miR-130b, miR-301a and miR-130a (Fort et al., 2018). As an oncomiR with major involvement in cancer, miR-301b levels change in response to hypoxia and can be dramatically up-regulated in the event of hypoxia in prostate cancer cells (Wang et al., 2016a,b). A previous study revealed that hypoxia induces autophagy, which then promotes cell survival in the presence of hypoxia, protecting the prostate cancer cells and therefore, facilitating their proliferation (Chhipa et al., 2011; Ma et al., 2014). In addition, hypoxia has the ability to up-regulate the expression of miR-301b, thus promoting the autophagy and viability of prostate cancer cells (Guo et al., 2016). On the basis of aforementioned evidence, we hypothesize that hypoxia-induced miR-301b-3p might be involved in the development of prostate cancer via interaction with LRP1B.

## 2. Methods and materials

### 2.1. Ethics statement

The study protocol was approved by the Ethics Committee of The Affiliated Hospital of Inner Mongolia Medical University. The clinical data of all patients were obtained from the medical records, and informed written consent was obtained from each patient. All experiments in the present study were conducted in strict accordance with the Helsinki declaration. Extensive efforts were made to ensure minimal suffering of the animals when conducting this study.

### 2.2. Microarray-based analysis

The prostate cancer microarray dataset GSE30994 was retrieved from the Gene Expression Omnibus (GEO) database (https://www.ncbi.nlm.nih.gov/geo/) with “prostate cancer” used as the key word. R language was used to perform differential analysis, and the differentially expressed genes (DEGs) were screened with $|\log2 \text{ fold change (FC)}| > 2$ and $p\ value < .05$ used as threshold values. Afterwards, the DEGs heat map was plotted.

### 2.3. Study subjects

A total of 124 human prostate cancer tissue specimens were obtained from patients admitted to the Affiliated Hospital of Inner Mongolia Medical University between December 2014 and October 2016 for the present study. The patients with the following conditions were excluded: (1) history of other malignancies, (2) severe infection, (3) cognitive impairment, (4) poor compliance. The tissue specimens were divided into two parts, with one part stored in liquid nitrogen at −80 °C and subjected to RNA and protein extraction, while the other part was fixed with paraformaldehyde and embedded in paraffin for subsequent experiments. All patients had not undergone radiotherapy or other treatments prior to the surgery.

### 2.4. Cell treatment

Human prostate cancer cell lines (DU145, PC-3, LNCaP and IA8) and human prostatic hyperplasia cell line (BPH-1) were purchased from BeNa Biology (Beijing, China). BPH-1 cells were cultured in LHC-9 (Biofluids Inc., Rockville, MD, USA) containing 0.5 ng/mL recombinant epidermal growth factor (EGF), 500 ng/mL hydrocortisone, 0.035 ng/mL bovine pituitary extract, 500 mmol/L ethanolamine, 500 nmol/L phosphoethanolamine, 0.01 mg/mL epinephrine and 0.1 ng/mL retinoic acid. In addition, DU145 cells were cultured in Roswell Park Memorial Institute (RPMI) 1640 medium (Gibco Company, Grand Island, NY, USA) containing 10% 0.11 g/L sodium pyruvate, 1.5 g/L $NaHCO_3$ and 2.5 g/L glucose. All cell lines were cultured in 5% $CO_2$ at 37 °C. When cell confluence reached 90%, the cells were counted, passaged, and screened with the use of reverse transcription quantitative polymerase chain reaction (RT-qPCR).

The cells with induced hypoxia were cultured in the Billups-Rotenburg room (Billups-Rothenberg, Inc., Del Mar, CA, USA) containing 1% $O_2$, 94% $N_2$ and 5% $CO_2$.

Next, the cells were transfected with plasmids of miR-301b-3p inhibitor, miR-301b-3p mimic, miR-301b-3p mimic + LRP1B-overexpression (OE), and miR-301b-3p inhibitor + si-LRP1B as well as their corresponding controls. Plasmids of miR-301b-3p inhibitor, miR-301b-3p mimic, si-LRP1B, and LRP1B-OE were all purchased from Guangzhou, RiboBio Co., Ltd. (Guangdong, China). The cells were then inoculated in a 24-well plate in accordance with the instructions provided on the Lipofectamine™ (Invitrogen, Carlsbad, California, USA).

### 2.5. RNA isolation and quantitation

Prostate cells at logarithmic growth phase were collected in order to conduct total RNA extraction with the use of Trizol (15596026, Invitrogen, Carlsbad, California, USA). The extracted RNA was reverse transcribed into complementary DNA (cDNA) according to the instructions provided on the PrimeScript reverse transcription reagent kit (RR047A, Takara Bio Inc., Otsu, Shiga, Japan). Primers (Table 1) were synthesized by Shanghai Sangon Biotechnology Co., Ltd. (Shanghai, China). RT-qPCR experiments were performed using 7500-type real-time PCR (ABI Company, Oyster Bay, NY, USA). The fold changes were then calculated using the $2^{-\triangle\triangle Ct}$ method.

### 2.6. Western blot analysis

Cells were lysed by radioimmunoprecipitation assay (RIPA) lysis (P0013B, Beyotime Biotechnology Co., Shanghai, China) and the total protein was collected. The protein quantity was determined with the use of a Bio-Rad Dc protein assay kit (Yuwei Biotechnology Instrument Co., Ltd., Guangzhou, China). Next, the protein was separated using sodium dodecyl sulfate-polyacrylamide gel electrophoresis (SDS-PAGE) and transferred onto a polyvinylidene fluoride membrane. Subsequently, the membrane was immersed in 1 × tris-buffered saline with tween 20 (TBST) containing 5% skimmed milk powder and shaken

**Table 1**
Primer sequence for RT-qPCR.

| Gene | Forward primer | Reverse primer |
|---|---|---|
| miR-301b-3p | 5′-TGCTGCTAACGAATGCTCTGA-3′ | 5′-CTCTGCTTTCAGATGCTTTGAC -3′ |
| LRP1B | 5′-TTCCCTTCTTACGCAACGGT-3′ | 5′-GGGAAATGGTTTCCTCGGCT-3′ |
| GADPH | 5′-TGGGTGTGAACCACGAGAA-3′ | 5′-GGCATGGACTGTGGTCATGA −3′ |
| U6 | 5′-TGC GGGTGCTCGCTTCGGCAGC-3′ | 5′-CAGTGCAGGGTCCGAGGT-3′ |

Note: RT-qPCR, reverse transcription quantitative polymerase chain reaction; miR-301b-3p, microRNA-301b-3p; LRP1B, lipoprotein receptor-related protein 1B; GAPDH, glyceraldehyde-3-phosphate dehydrogenase.

gently at room temperature for 2 h. The membrane was then incubated overnight at 4 °C with the following primary antibodies purchased from Abcam Inc. (Cambridge, MA, USA): LRP1B (ab162688, 1:2000), HIF1-α (ab51608, 1:1000), matrix metalloproteinase (MMP) 2 (ab92536, 1:1000), MMP9 (ab38898, 1:1000), vascular endothelial growth factor (VEGF) (ab32152, 1:1000) and GAPDH (ab128915, 1:5000). After that, the membrane was incubated with secondary goat anti-rabbit immunoglobulin G (IgG) (ab6721, 1:20000, Abcam Inc., Cambridge, MA, USA) at room temperature for 1 h. Enhanced chemiluminescence (ECL) reagent and band intensities were quantified using Image J software (NIH free software) in order to visualize the immunocomplexes on the membrane.

### 2.7. 3-(4,5-dimethylthiazol-2-yl)-2,5-diphenyltetrazolium bromide (MTT) assay

The cells were seeded in a 96-well plate at a density of $3 \times 10^3$ cells/well. Next, 20 μL of MTT solution (5 mg/mL; Sigma-Aldrich Chemical Company, St Louis, MO, USA) was added to the plate and incubation was carried out for 4 h. Next, 200 μL of dimethyl sulfoxide (DMSO) (Sigma-Aldrich Chemical Company, St Louis, MO, USA) was added and the absorbance was measured at 490 nm with the use of a microplate reader (Bio Tek Instruments, Inc., Winooski, VT, USA).

### 2.8. Scratch test

The cell suspension ($2 \times 10^5$ cells/mL) was placed in a 6-well plate (2 mL/well), with the solution changed after 6 h. Prior to the solution being changed, a straight line was made in the center of each well. Next, the plate was washed 3 times by buffer for the removal of the suspended cells. Finally, each well was added with fresh pure Dulbecco's modified eagle's medium (DMEM). Photographs of the migration of cells were obtained at each time point under a microscope, and the healing rate of the scratches was recorded.

### 2.9. Transwell assay

The stem cells transfected for 24 h were washed by 200 μL serum-free 1640 medium, resuspended in serum-free DMEM medium, counted and diluted to a density of $3 \times 10^5$ cells/mL. The apical chamber coated with Matrigel (1:10, BD Biosciences, Franklin Lakes, NJ, USA) was dispensed with 100 μL cell suspension, while the basolateral chamber was added with 600 μL DMEM medium containing 10% serum (serum functions as chemokine). The experiment was performed in accordance with the instructions provided on the Transwell chamber and crystal violet was used for staining. Three fields of view were randomly selected and the number of cells across the membrane was counted.

### 2.10. Dual luciferase reporter gene assay

The 3′-untranslated region (3′UTR) of LRP1B was cloned and introduced into pmirGLO (E1330, Promega Corporation, Madison, WI, USA) luciferase vector. The correctly sequenced luciferase reporter plasmids LRP1B-wild type (WT) and LRP1B-mutant (MUT) were respectively co-transfected with miR-301b-3p into HEK-293T cells (Beinuo Biotechnology Co., Ltd., Shanghai, China). The cells were subsequently collected and lysed following a 48 h transfection. The luciferase activity was detected using a luciferase assay kit.

### 2.11. Tumor xenograft in nude mice

Human prostate cancer cell line DU145 was collected, and made into single cell suspension, followed by resuspension by the mixture of PBS and Matrigel (1:1) with the final cell concentration diluted to $1 \times 10^6$ cells/200 μL. A total of 42 nude mice were injected with cells transfected with miR-301b-3p mimic, miR-301b-3p inhibitor, miR-301b-3p mimic + LRP1B-OE, miR-301b-3p inhibitor + si-LRP1B, miR-301b-3p inhibitor + LRP1B-OE or corresponding controls. A total of $1 \times 10^6$ (200 μL) cells were subcutaneously inoculated into the back of the right hind leg of nude mice, after which the mice were kept in the same environment and observed every 7 days. The length and width of the tumor were recorded with the tumor volume calculated using the following formula: tumor volume = length × width $^2/2$. Afterwards, a curve illustrating tumor growth was plotted. Finally, the nude mice were euthanized on the 35th day and the tumors were dissected, with three tumors obtained from each group.

### 2.12. Statistical analysis

SPSS 21.0 statistical software (IBM Corp. Armonk, NY, USA) was employed for of statistical analysis. The measurement data were expressed as mean ± standard deviation. Paired *t*-test was used for the comparisons between two paired groups with normal distribution and inhomogeneity of variance, while unpaired *t*-test was used for the comparison between two unpaired groups. Data comparisons among multiple groups were performed using one-way analysis of variance (ANOVA), followed by a Tukey multiple comparisons posttest. Pearson's correlation coefficient was used for the analysis of the correlation between the expression of miR-301b-3p and LRP1B. Statistical analysis in relation to time-based measurements was conducted using ANOVA of repeated measurements, followed by a Bonferroni post hoc test for multiple comparisons. A value of $p < .05$ was considered as statistically significant.

## 3. Results

### 3.1. Expression of LRP1B is altered in prostate cancer

Analysis of microarray data GSE30994 revealed that LRP1B was the most obvious DEG and was down-regulated in prostate cancer (Fig. 1A). LRP1B has been identified to be one of the 10 most significant genes that have been found to be absent in human cancer samples (Prazeres et al., 2011), but its upstream regulatory mechanisms remain unclear. We employed TargetScan (http://www.targetscan.org/vert_71/), starBase (http://starbase.sysu.edu.cn/index.php) and miRWalk (http://mirwalk.umm.uni-heidelberg.de/) to predict the potential miRNAs binding to LRP1B and we found that there were three intersections (hsa-miR-301b-3p, hsa-miR-3666 and hsa-miR-454-3p) (Fig. 1B). Among them, miR-3666 and miR-454-3p were anti-oncogenes, while miR-301b was significantly up-regulated in cancer (Egawa et al., 2016). Therefore, miR-301b-3p was selected for subsequent experiment. A study has verified that hypoxia can enhance miR-301b expression (Yuile and Tran, 2002). The aforementioned results suggested that hypoxia-induced miR-301b-3p affects the development of prostate cancer by regulating LRP1B.

### 3.2. miR-301b-3p is highly expressed in prostate cancer

RT-qPCR was performed to test the expression of miR-301b-3p in 124 prostate cancer tissues and normal adjacent tissues to investigate the changes in the expression of miR-301b-3p in prostate cancer. The results revealed that miR-301b-3p expression was significantly higher in prostate cancer tissues than that in normal adjacent tissues ($p < .05$; Fig. 2A). In addition, further experiment verified that compared with normal prostatic hyperplasia cell line BPH-1, there was a high expression in miR-301b-3p in prostate cancer cell lines DU145, PC-3, LNCaP and IA8 ($p < .05$) (Fig. 2B), among which DU145 presented with the highest miR-301b-3p expression. The above results suggest that the expression of miR-301b-3p was up-regulated in prostate cancer and hence, DU145 and PC-3 cell lines were selected for subsequent experiments.

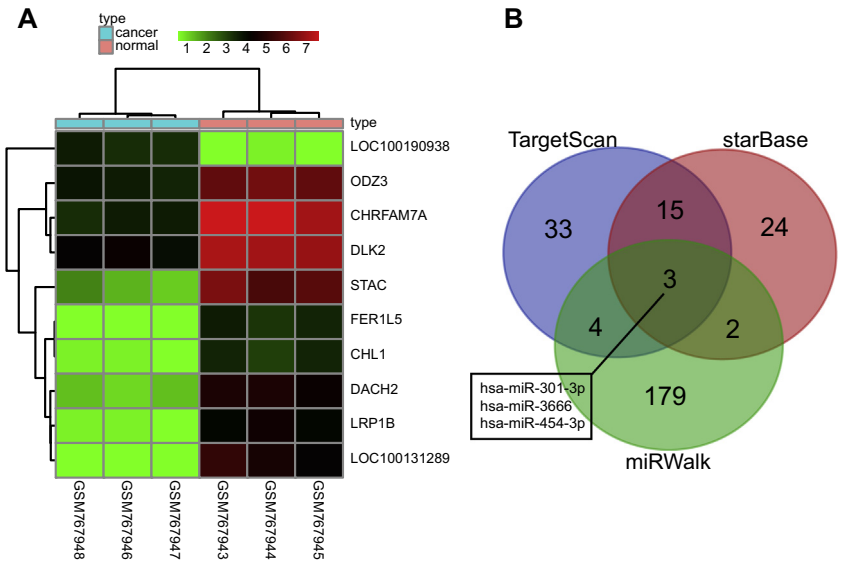


**Fig. 1.** Hypoxia-induced miR-301b-3p affects the development of prostate cancer by regulating LRP1B. Screening of the DEGs in GSE30994 dataset (A). The abscissa represents the sample number and the ordinate represents DEGs. The histogram at the upper right refers to color gradation, and each rectangle in the figure corresponds to a sample expression value. Potential miRNAs binding to LRP1B predicted by bioinformatics websites (B).

### *3.3. Hypoxia induces a higher expression of miR-301b-3p in prostate cancer cells*

It has been reported that hypoxia can lead to an increase in the expression of miR-301b (Wu et al., 2016). HIF1-α is the major transcription factor that regulates the expression of downstream target genes in response to hypoxia (Wang et al., 2016a,b). In our experiment, prostate cancer cells DU145 and PC-3 received treatment with 1% oxygen or dimethyloxalylglycine (DMOG) (a mature drug used to mimic hypoxic conditions). Next, the protein content of HIF1-α in each group was analyzed using western blot analysis. As shown in Fig. 3A, the protein content of HIF1-α in DU145 and PC-3 cells treated with hypoxia or DMOG was higher than that in normal prostatic hyperplasia cells ($p < .05$). This was indicative of the successful establishment of the hypoxia model.

Subsequently, RT-qPCR was conducted to measure the expression of miR-301b-3p (Fig. 3B) and LRP1B (Fig. 3C) in DU145 and PC-3 cells, the results of which demonstrated that in DU145 and PC-3 cells treated with hypoxia or DMOG, there was an increase in the expression of miR-301b-3p ($p < .05$) and a decrease in LRP1B mRNA expression ($p < .05$) when compared with normal prostatic hyperplasia cells. Next, the expression of HIF1-α in DU145 and PC-3 cells was down-regulated with the use of shRNA under hypoxic conditions. Following western blot analysis, it was found that the HIF1-α protein content in DU145 and PC-3 cells treated with shRNA was much lower than that in normal prostatic hyperplasia cells under hypoxic conditions ($p < .05$; Fig. 3D). Finally, the expression of miR-301b-3p in DU145 and PC-3 cells after HIF1-α knockdown was detected using RT-qPCR under hypoxic conditions. The results showed that the expression of miR-301b-3p was decreased in DU145 and PC-3 cells treated with sh-HIF1-α ($p < .05$; Fig. 3E). It was demonstrated that there was a significant reduction in the expression of miR-301b-3p when HIF1-α was down-regulated. Collectively, these results provided verification that hypoxia can lead to the enhancement of miR-301b-3p expression in prostate cancer cells.

### *3.4. Up-regulated miR-301b-3p accelerates the viability, migration and invasion of prostate cancer cells*

To clarify the effect of miR-301b-3p on the biological function of

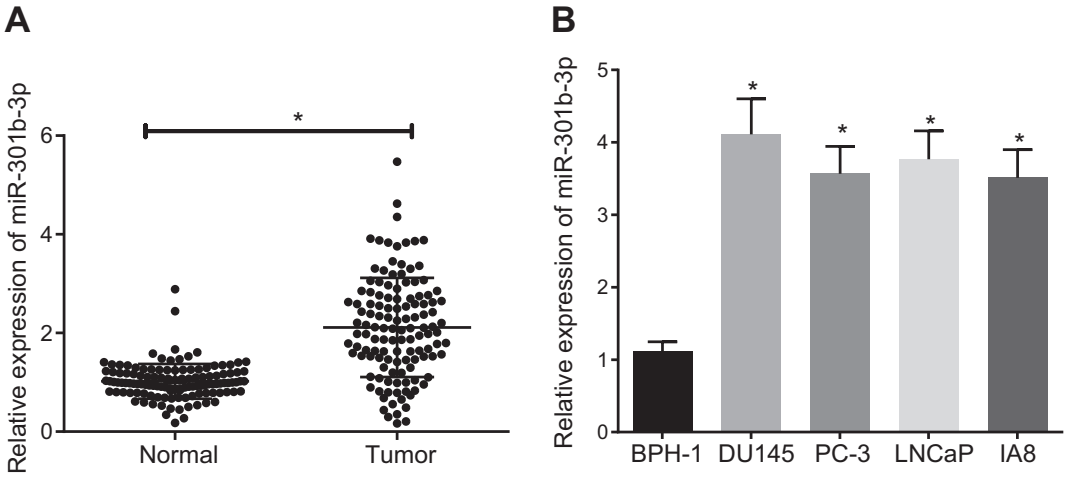


**Fig. 2.** miR-301b-3p presents with high expression in prostate cancer. The relative expression of miR-301b-3p in 124 prostate cancer tissues and normal adjacent tissues detected by RT-qPCR (A). The relative expression of miR-301b-3p in normal prostatic hyperplasia cells and human prostate cancer cell lines detected by RT-qPCR (B). The data were measurement data and expressed as mean ± standard deviation. $p < .05$ means significant difference, $^{*}p < .05$ vs. normal adjacent tissues or BPH-1 cells. Paired *t*-test was used for comparison between two groups, and one-way ANOVA was used for comparison among multiple groups, followed by a Tukey multiple comparisons posttest. n = 124. The experiment was repeated three times independently.

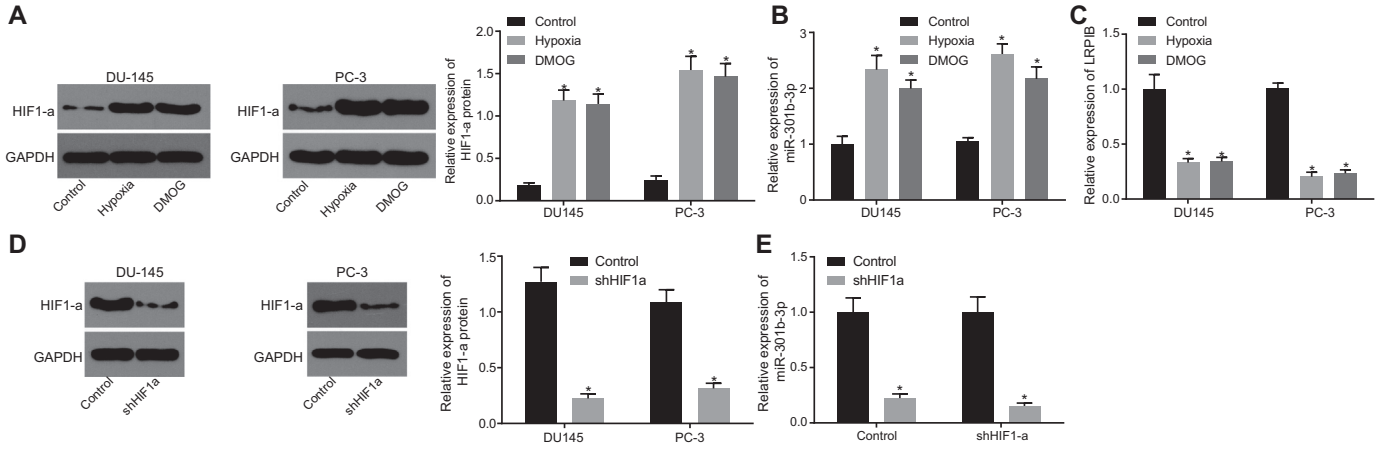


**Fig. 3.** Hypoxia elicits increased expression of miR-301b-3p in prostate cancer cells. Western blot analysis of HIF1-α protein in DU145 and PC-3 cells treated with hypoxia or DMOG (A). The relative expression of miR-301b-3p in DU145 and PC-3 cells treated with hypoxia or DMOG measured by RT-qPCR (B). The mRNA expression of LRP1B in DU145 and PC-3 cells treated with hypoxia or DMOG measured by RT-qPCR (C). Western blot analysis of HIF1-α protein in DU145 and PC-3 cells (D). The expression of miR-301b in DU145 and PC-3 cells treated with sh-HIF1-α detected by RT-qPCR (E). The data were measurement data and expressed as mean ± standard deviation. $p < .05$ means significant difference, $^{*}p < .05$ vs. mimic normal cells. Unpaired *t*-test was used for comparison between two groups, and one-way ANOVA was used for comparison among multiple groups, followed by a Tukey multiple comparisons posttest. The experiment was repeated three times independently.

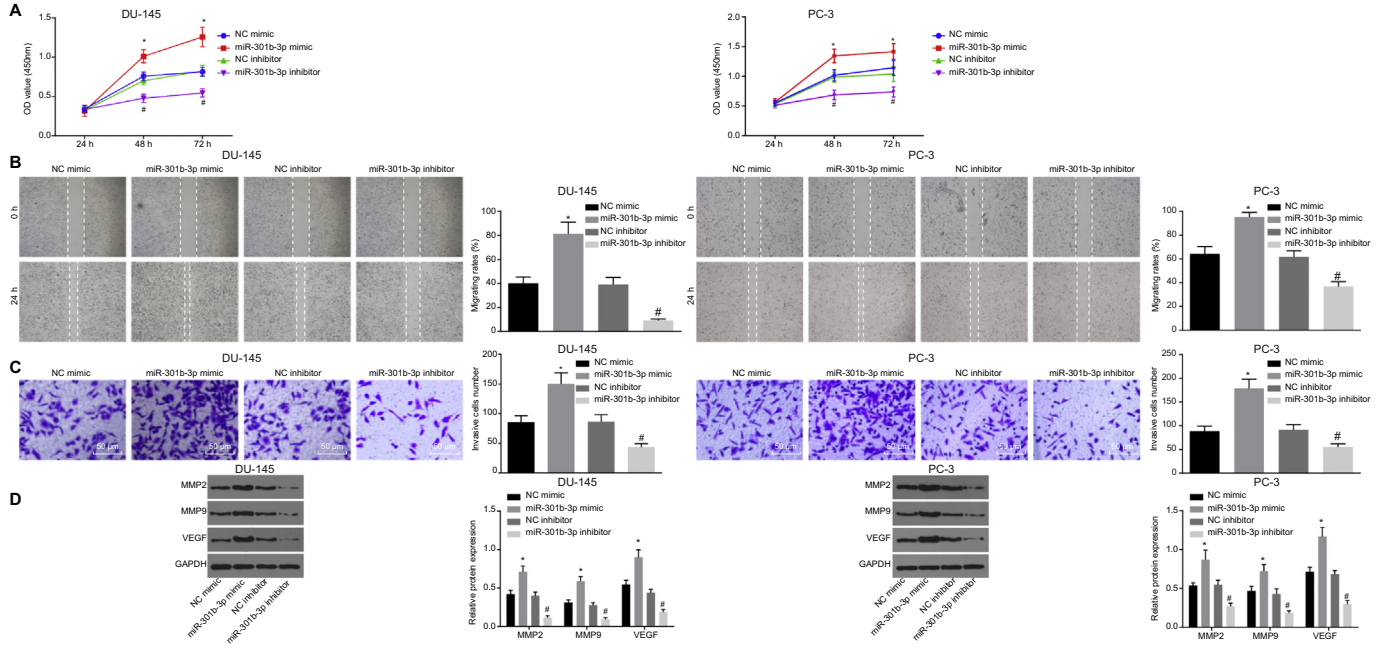


**Fig. 4.** The viability, migration and invasion of prostate cancer cells are promoted by miR-301b-3p overexpression. The viability ability of DU145 and PC-3 cells detected by MTT assay (A). The migration ability of DU145 and PC-3 cells detected by scratch test (B). The invasion ability of DU145 and PC-3 cells detected by Transwell assay (C). Western blot analysis of migration- and invasion-associated proteins in DU145 and PC-3 cells (D). The data were measurement data and expressed as mean ± standard deviation. $p < .05$ means significant difference, $^{*}p < .05$ vs. cells transfected with NC, $^{\#}p < .05$ vs. cells transfected with NC inhibitor. Unpaired *t*-test was used for comparison between two groups. Statistical analysis in relation to time-based measurements was realized using ANOVA of repeated measurements, followed by a Bonferroni post hoc test for multiple comparisons. The experiment was repeated three times independently.

prostate cancer cells, we conducted a series of experiments in prostate cancer cell lines DU145 and PC-3. Firstly, the viability of DU145 and PC-3 cells was detected with the use of MTT assay. The results showed (Fig. 4A) that there was an increase in the number of cells in each group with time. However, at 24, 48, and 72 h, the viability of cells transfected with miR-301b-3p mimic was increased ($p < .05$) and that of cells transfected with miR-301b-3p inhibitor was markedly decreased ($p < .05$).

The migration ability of DU145 and PC-3 cells was then tested by scratch test. The results showed that there was an increase in the migration ability of cells transfected with miR-301b-3p mimic ($p < .05$), while that of cells transfected with miR-301b-3p inhibitor was inhibited ($p < .05$; Fig. 4B).

Moreover, the results from the Transwell assay that was conducted to test the invasive ability of DU145 and PC-3 cells (Fig. 4C) revealed that there was an increase in invasion ability in the cells transfected with miR-301b-3p mimic ($p < .05$), while that of cells transfected with miR-301b-3p inhibitor was decreased ($p < .05$). The results from western blot analysis (Fig. 4D) showed that there was an up-regulation in the expression of migration- and invasion-related proteins (MMP2,

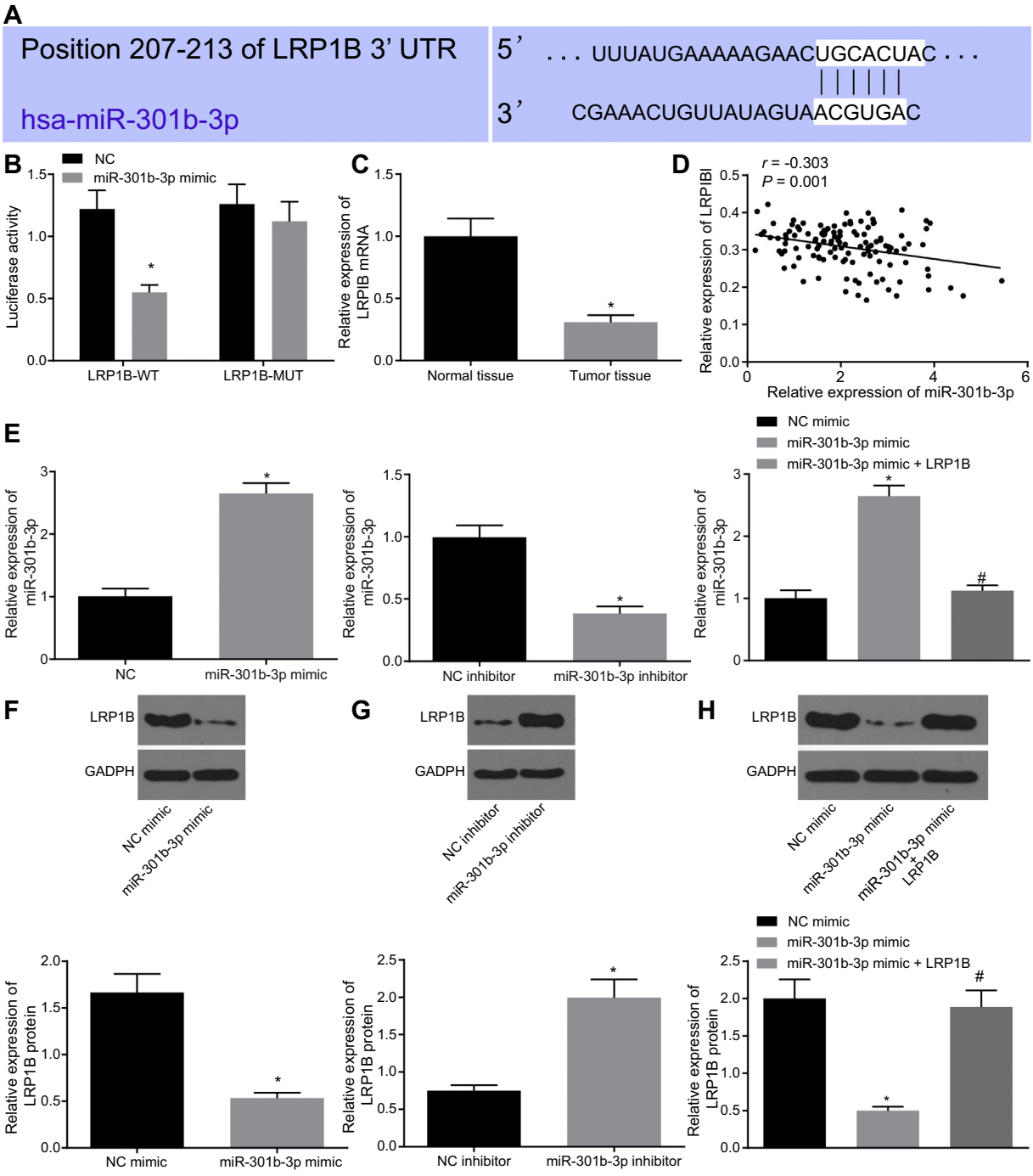


**Fig. 5.** LRP1B is a target gene of miR-301b-3p and can be negatively regulated by miR-301b-3p. The predicted binding site of miR-301b-3p to LRP1B by the biological website (A). The fluorescence activity of miR-301b-3p and LRP1B (B). The mRNA expression of LRP1B in prostate cancer tissues measured by RT-qPCR (C). Correlation analysis between miR-301b-3p and LRP1B (D). miR-301b-3p expression in DU145 and PC-3 cells detected by RT-qPCR (E). Western blot analysis of LRP1B protein in DU145 and PC-3 cells (F and H). The data are measurement data, and expressed as mean ± standard deviation. $p < .05$ means significant difference, $^{*}p < .05$ vs. cells transfected with NC or NC inhibitor, $^{\#}p < .05$ vs. cells transfected with miR-301b-3p mimic. Unpaired *t*-test was used for comparison between two groups, and one-way ANOVA was used for comparison among multiple groups, followed by a Tukey multiple comparisons posttest. Pearson's correlation coefficient was used to analyze the correlation between the expression of miR-301b-3p and LRP1B. The experiment was repeated three times independently.

MMP9, and VEGF) in DU145 and PC-3 cells transfected with miR-301b-3p mimic ($p < .05$) while it was decreased in following transfection with miR-301b-3p ($p < .05$). The aforementioned results verified that overexpression of miR-301b-3p can promote the viability, migration and invasion of prostate cancer cells.

### 3.5. LRP1B is a target gene of miR-301b-3p

The biological website TargetScan available at http://www.targetscan.org/vert_71/ revealed a potential binding site between miR-301b-3p and LRP1B (Fig. 5A), which was further verified by dual luciferase reporter gene assay (Fig. 5B), which showed that the luciferase activity of LRP1B-WT was inhibited by miR-301b-3p mimic ($p < .05$), while that of LRP1B-MUT remained unaffected in response

to miR-301b-3p mimic ($p > .05$). These results suggest that miR-301b-3p can target LRP1B. In addition, the results from RT-qPCR showed that there was a downregulation in LRP1B in prostate cancer tissues (Fig. 5C). Correlation analysis showed that there exists a negative correlation between miR-301b-3p and LRP1B (Fig. 5D).

Subsequently, DU145 and PC-3 cells were further transfected with miR-301b-3p mimic, miR-301b-3p inhibitor or the corresponding controls, and RT-qPCR was conducted in order to detect the expression of miR-301b-3p following different transfections. As shown in Fig. 5E, there was an increase in the expression of miR-301b-3p in miR-301b-3p mimic-transfected cells ($p < .05$). In comparison with miR-301b-3p mimic + LRP1B-OE transfection, there was no significant difference in the expression of miR-301b-3p following miR-301b-3p mimic transfection ($p > .05$), while the expression of miR-301b-3p in miR-301b-3p inhibitor-transfected cells was decreased ($p < .05$).

Subsequent western blot analysis results (Fig. 5F–H) revealed that there was an up-regulation in the expression of LRP1B protein in DU145 and PC-3 cells transfected with miR-301b-3p inhibitor ($p < .05$), which was evidently down-regulated following miR-301b-3p mimic transfection ($p < .05$). However, LRP1B protein expression in DU145 and PC-3 cells transfected with miR-301b-3p mimic + LRP1B-OE was increased in comparison to that of the miR-301b-3p mimic transfection ($p < .05$). The aforementioned findings provided evidence that the overexpression of LRP1B can reverse the decrease of LRP1B expression induced by up-regulated miR-301b-3p.

### 3.6. Overexpressed miR-301b-3p stimulates proliferation, migration and invasion of prostate cancer cells through LRP1B inhibition

To elucidate whether LRP1B can reverse the effects of miR-301b-3p on the proliferation, migration and invasion of prostate cancer cells, DU145 and PC-3 cells were further transfected with inhibitor NC + si-NC, inhibitor NC + si-LRP1B, miR-301b-3p inhibitor + si-NC and miR-301b-3p inhibitor + si-LRP1B, after which RT-qPCR was conducted to detect the expression of miR-301b-3p in prostate cancer upon different transfections. The results showed no significant difference in miR-301b-3p expression between inhibitor NC + si-NC transfection and inhibitor NC + si-LRP1B transfection. However, following miR-301b-3p inhibitor + si-NC and miR-301b-3p inhibitor + si-LRP1B transfection, there was a decrease in the expression of miR-301b-3p ($p < .05$; Fig. 6A).

MTT assay was performed to detect the viability of DU145 and PC-3 cells. As illustrated in Fig. 6B, the viability of cells was enhanced with time. At 24 h, 48 h, and 72 h, the viability of cells transfected with inhibitor NC + si-LRP1B was increased ($p < .05$), while it was reduced upon miR-301b-3p inhibitor + si-NC transfection ($p < .05$) in comparison with inhibitor NC + si-NC transfection. There was no evident difference observed in the viability of cells transfected with miR-301b-3p inhibitor + si-LRP1B ($p > .05$).

The migration and invasion abilities of DU145 and PC-3 cells were detected with the use of the Scratch test and Transwell assay. As depicted in Fig. 6C & D, in comparison with inhibitor NC + si-NC transfection, inhibitor NC + si-LRP1B transfection resulted in an increase in the number of migration and invasion cells while cells transfected with miR-301b-3p inhibitor + si-NC showed reduced migration and invasion abilities ($p < .05$). There were no significant changes observed regarding migration and invasion abilities of cells following transfection with miR-301b-3p inhibitor + si-LRP1B ($p > .05$). There was more significant enhancement in the migration and invasion abilities of cells in response to miR-301b-3p inhibitor + si-LRP1B transfection compared to transfection with miR-301b-3p inhibitor ($p < .05$).

The results from western blot analysis (Fig. 6E) revealed that in comparison with inhibitor NC + si-NC transfection, inhibitor NC + si-LRP1B transfection resulted in up-regulated expression of MMP2, MMP9 and VEGF in DU145 and PC-3 cells transfected with inhibitor NC + si-LRP1B ($p < .05$) while miR-301b-3p inhibitor + si-NC transfection presented with reduced expression of MMP 2, MMP9 and VEGF ($p < .05$). In cells transfected with miR-301b-3p inhibitor + si-LRP1B, there was no significant difference in the expression of MMP 2, MMP9 and VEGF in comparison with inhibitor NC + si-NC transfection ($p > .05$). The aforementioned factors were all increased in miR-301b-3p inhibitor + si-LRP1B-transfected cells as compared with miR-301b-3p inhibitor + si-NC transfection ($p < .05$). These results verified that overexpression of miR-301b-3p can promote proliferation, migration and invasion abilities of prostate cancer cells through LRP1B suppression.

### 3.7. Overexpressed miR-301b-3p promotes tumor growth via suppressing LRP1B in vivo

The results from the tumor xenograft in nude mice (Fig. 7) demonstrated that there was an increase in tumor weight and volume with time ($p < .05$). Tumor weight and volume were increased in mice injected with cells transfected with miR-301b-3p mimic and presented with the fastest speed ($p < .05$), which was blocked by miR-301b-3p mimic + LRP1B-OE treatment ($p < .05$). Moreover, the mice injected with miR-301b-3p inhibitor presented with a decrease in tumor volume and weight and a slower speed ($p < .05$), while these factors were increased in mice injected with cells transfected with miR-301b-3p inhibitor + si-LRP1B ($p < .05$). Both treatment of miR-301b-3p inhibitor and LRP1B-OE resulted in the most significant reduction in tumor volume and weight ($p < .05$). These results indicate that overexpression of miR-301b-3p could accelerate tumor growth in mice through the negative regulation of LRP1B.

## 4. Discussion

Prostate cancer is one of the leading causes of cancer-related deaths in adult men, which is partly due to its tremendous biological heterogeneity (Taylor et al., 2010; von Eyben et al., 2018). The incidence of prostate cancer has raised worldwide concern in recent years, due to the high mortality rate, which is continuously growing with time (Huang et al., 2018). Previous studies have identified miRNAs as practicable and promising biomarkers for prostate cancer (Fendler et al., 2011). In the present study, a series of in vitro and in vivo experiments were conducted with aims of investigating hypoxia-induced miR-301b-3p and its influence on prostate cancer by targeting LRP1B. The findings obtained suggested that hypoxia can up-regulate miR-301b-3p to antagonize LRP1B, thereby promoting cell proliferation, migration and invasion in prostate cancer.

Our results revealed that there was a higher expression in miR-301b-3p in prostate cancer tissues and cells. It was concluded from a comprehensive data analysis that has-miR-301b is highly expressed in prostate cancer and involves in its pathogenesis (Fort et al., 2018). The up-regulation in miR-301b expression has also been detected in lung cancer cell lines and tissues, and a high expression in miR-301b results in the acceleration of tumorigenesis in lung cancer (Wu et al., 2016). Moreover, there is a high expression of both miR-301a and miR-301b in prostate cancer (Nam et al., 2016). A previous study revealed that miR-301b was up-regulated in bladder cancer tissues compared with normal adjacent tissues (Yan et al., 2017).

Another finding from our study suggests that hypoxia leads to the significant upregulation of miR-301b-3p in prostate cancer cells. This was previously verified in a study, which showed that two co-existing conditions of hypoxia and low androgen are always found in prostate cancer tissues following medical or surgical castration (Chhipa et al., 2011). miR-301a/b is one of the hypoxia-responsive miRNAs, and its expression has been found to be dramatically promoted by hypoxia and enhanced miR-301a/b could lead to the suppression of autophagy of prostate cancer cells under a low oxygen condition and promote radioresistance of prostate cancer cells (Guo et al., 2016, Wang et al., 2016a,b). All of the aforementioned studies verified that hypoxia can

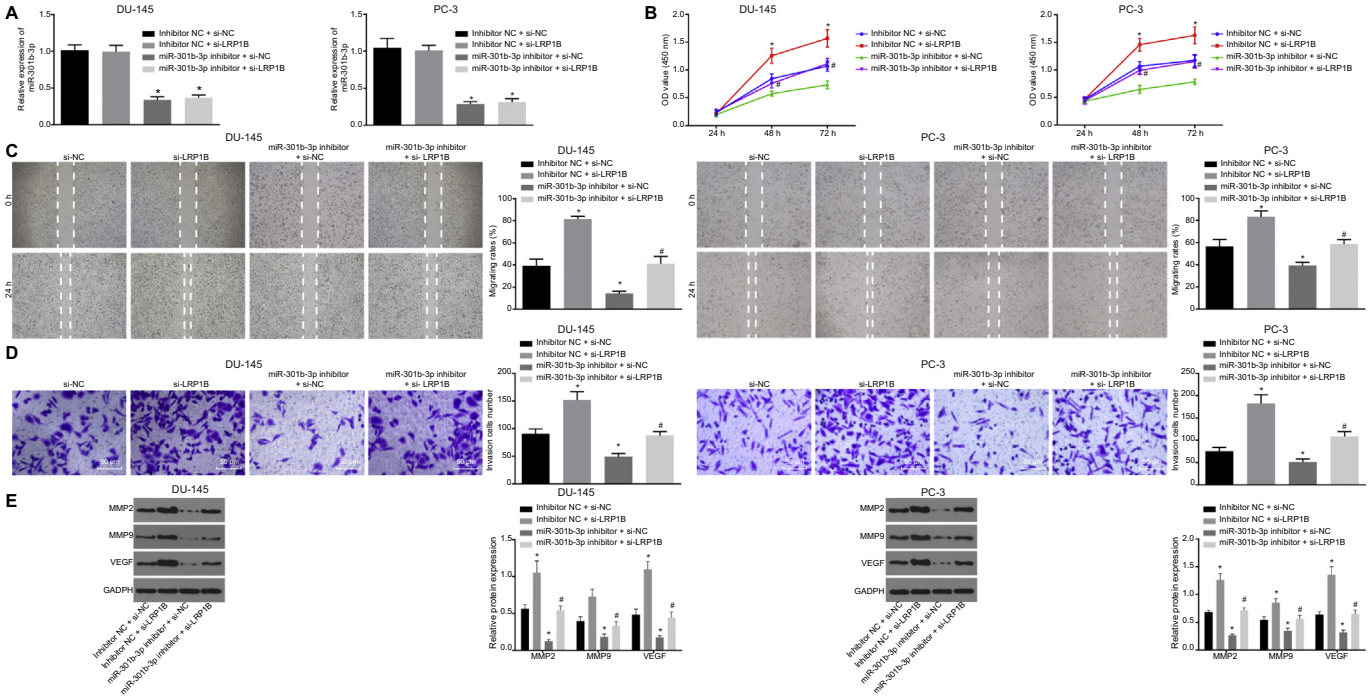

**Fig. 6.** The viability, migration and invasion of prostate cancer cells are promoted by hypoxia-induced miR-301b-3p via targeting LRP1B. miR-301b-3p expression in DU145 and PC-3 cells detected by RT-qPCR (A).The viability of DU145 and PC-3 cells detected by MTT assay (B). The migration ability of DU145 and PC-3 cells measured using scratch test (C). The invasive ability of DU145 and PC-3 cells measured using Transwell assay (D). Western blot analysis of cell migration- and invasion-associated proteins in DU145 and PC-3 cells (E). The data were measurement data and expressed as mean ± standard deviation. $p < .05$ means significant difference, $^{*}p < .05$ vs. cells transfected with si-NC; $^{\#}p < .05$ vs. cells transfected with miR-301b-3p inhibitor + si-NC. Unpaired *t*-test was used for comparison between two groups. Statistical analysis in relation to time-based measurements was realized using ANOVA of repeated measurements, followed by a Bonferroni post hoc test for multiple comparisons. One-way ANOVA was used for comparison among multiple groups, followed by a Tukey multiple comparisons posttest. The experiment was repeated three times independently.

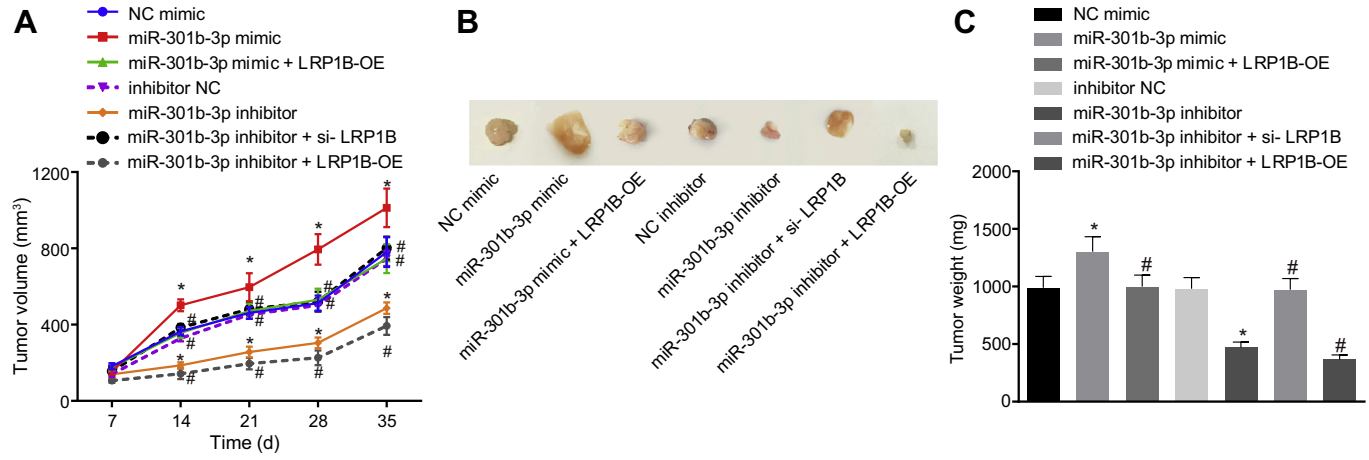

**Fig. 7.** miR-301b-3p promotes tumor growth by inhibiting LRP1B. Xenograft tumors and quantitative analysis of tumor volume and weight (A and C). The data were measurement data, and expressed as mean ± standard deviation. $p < .05$ means significant difference. $^{*}p < .05$ vs. mice injected with cells transfected with NC, $^{\#}p < .05$ vs. mice injected with cells transfected with miR-301b-3p mimic or miR-301b-3p inhibitor. Statistical analysis in relation to time-based measurements was realized using ANOVA of repeated measurements, followed by a Bonferroni post hoc test for multiple comparisons. One-way ANOVA was used for comparison among multiple groups, followed by a Tukey multiple comparisons posttest. n = 6. The experiment was repeated three times independently.

give rise to an increase in the expression of miR-301b in prostate cancer cells.

Furthermore, the bioinformatics prediction website in combination with dual luciferase reporter gene assay revealed that LRP1B was the target gene of miR-301b-3p. Consistently, miR-603 down-regulates LRPAP1 mRNA and protein levels by directly binding to the 3′-UTR of LRPAP1 (Zhang et al., 2016). Moreover, the invasive and growth capacity of cancer cells can be conferred as the expression of LRP1B, which is suppressed when there is a higher expression of miR-548a-5p, which is promoted by genomic gain (Prazeres et al., 2011). Previous studies have provided evidence that LRP1B has tumor suppressive properties in several kinds of cancer. For example, the knock-down of LRP1B by shRNA can significantly potentiate cell invasion and migration, as well as anchorage-independent growth in renal cancer cells 127 and HEK293 cells in vitro (Ni et al., 2013). In addition, down-regulated levels of LRP1B in colon cancer promote the growth and migration of

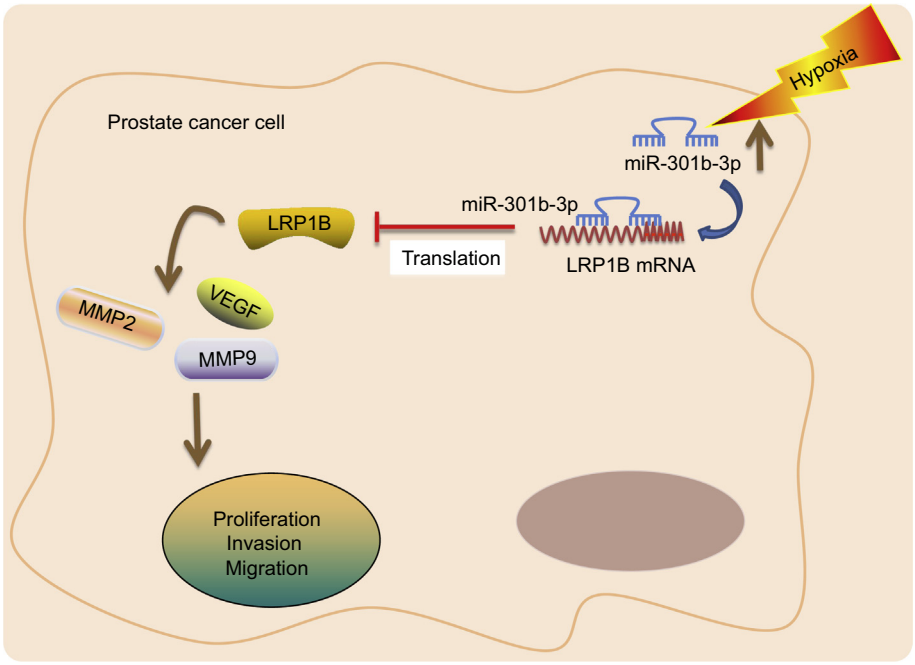


**Fig. 8.** Hypoxia-induced miR-301b-3p promotes the proliferation, migration and invasion of prostate cancer cells by targeting LRP1B.

cancer cells (Wang et al., 2017). As illustrated in a previous study, MMP2, MMP9 and VEGF genes have major involvement in cell migration and invasion in prostate cancer (Moroz et al., 2013; Kim et al., 2013). miR-204-5p suppresses cell proliferation, migration and invasion in melanoma through MMP9 inhibition (Luan et al., 2017). miR-29b-3p-mediated MMP2 inhibition prevents the progression of arterial calcification (Jiang et al., 2017). VEGF acts to disrupt the metastasis of breast cancer cells and miR-20b has been found to reduce VEGF protein expression (Cascio et al., 2010). Damodaran et al. suggested that the overexpression of miR-301a leads to the activation of invasion and migration of prostate cancer cells (Damodaran et al., 2016). Therefore, we came to the conclusion that overexpressed miR-301b-3p can enhance proliferation, migration and invasion abilities of prostate cancer cells through LRP1B inhibition.

The effect of miR-301b-3p on prostate cancer was further verified by conducting an in vivo experiment, the results of which demonstrated that miR-301b-3p promoted tumor growth in mice by downregulating LRP1B. A previous study found the same results, indicating that a high expression of miR-301a can potentiate the growth of xenograft tumors by directly targeting the tumor suppressor p63 in prostate cancer (Nam et al., 2016).

## 5. Conclusion

In conclusion, hypoxia induced miR-301b-3p up-regulation could potentially antagonize the expression of LRP1B, thereby promoting proliferation, migration and invasion of prostate cancer cells (Fig. 8). This investigation yields a better understanding of the in-depth mechanisms regarding LRP1B and miR-301b-3p and their function in prostate cancer cells, potentially providing important therapeutic implications in prostate cancer.

## Authors' contributions

Haiying Zheng and Ligang Bai designed the study. Ligang Bai collated the data, carried out data analyses and produced the initial draft of the manuscript. Haiying Zheng contributed to drafting the manuscript. All authors have read and approved the final submitted manuscript.

## Declaration of Competing Interest

None.

## Acknowledgments

We would like to acknowledge the reviewers for their helpful comments on this paper.

## References

Cascio, S., D'Andrea, A., Ferla, R., Surmacz, E., Gulotta, E., Amodeo, V., Bazan, V., Gebbia, N., Russo, A., 2010. miR-20b modulates VEGF expression by targeting HIF-1 alpha and STAT3 in MCF-7 breast cancer cells. J. Cell. Physiol. 224, 242–249.
Chang, L., Graham, P.H., Hao, J., Bucci, J., Cozzi, P.J., Kearsley, J.H., Li, Y., 2014. Emerging roles of radioresistance in prostate cancer metastasis and radiation therapy. Cancer Metastasis Rev. 33, 469–496.
Chen, W., Mao, K., Liu, Z., Dinh-Xuan, A.T., 2014. The role of the RhoA/Rho kinase pathway in angiogenesis and its potential value in prostate cancer (Review). Oncol. Lett. 8, 1907–1911.
Chhipa, R.R., Wu, Y., Ip, C., 2011. AMPK-mediated autophagy is a survival mechanism in androgen-dependent prostate cancer cells subjected to androgen deprivation and hypoxia. Cell. Signal. 23, 1466–1472.
Damodaran, C., Das, T.P., Papu John, A.M., Suman, S., Kolluru, V., Morris, T.J., Faber, E.N., Rai, S.N., Messer, J.C., Alatassi, H., Ankem, M.K., 2016. miR-301a expression: a prognostic marker for prostate cancer. Urol. Oncol. 34 (336), e313–e320.
Dietrich, M.F., van der Weyden, L., Prosser, H.M., Bradley, A., Herz, J., Adams, D.J., 2010. Ectodomains of the LDL receptor-related proteins LRP1b and LRP4 have anchorage independent functions in vivo. PLoS One 5, e9960.
Egawa, H., Jingushi, K., Hirono, T., Ueda, Y., Kitae, K., Nakata, W., Fujita, K., Uemura, M., Nonomura, N., Tsujikawa, K., 2016. The miR-130 family promotes cell migration and invasion in bladder cancer through FAK and Akt phosphorylation by regulating PTEN. Sci. Rep. 6, 20574.
Fendler, A., Jung, M., Stephan, C., Honey, R.J., Stewart, R.J., Pace, K.T., Erbersdobler, A., Samaan, S., Jung, K., Yousef, G.M., 2011. miRNAs can predict prostate cancer biochemical relapse and are involved in tumor progression. Int. J. Oncol. 39, 1183–1192.
Fort, R.S., Matho, C., Oliveira-Rizzo, C., Garat, B., Sotelo-Silveira, J.R., Duhagon, M.A., 2018. An integrated view of the role of miR-130b/301b miRNA cluster in prostate cancer. Exp. Hematol. Oncol. 7, 10.
Guo, Y.J., Liu, J.X., Guan, Y.W., 2016. Hypoxia induced upregulation of miR-301a/b contributes to increased cell autophagy and viability of prostate cancer cells by targeting NDRG2. Eur. Rev. Med. Pharmacol. Sci. 20, 101–108.
Huang, Y., Jiang, X., Liang, X., Jiang, G., 2018. Molecular and cellular mechanisms of castration resistant prostate cancer. Oncol. Lett. 15, 6063–6076.
Jiang, W., Zhang, Z., Yang, H., Lin, Q., Han, C., Qin, X., 2017. The involvement of miR-29b-3p in arterial calcification by targeting matrix Metalloproteinase-2. Biomed. Res.

Int. 2017, 6713606.
Kim, D.H., Hossain, M.A., Kim, M.Y., Kim, J.A., Yoon, J.H., Suh, H.S., Kim, G.Y., Choi, Y.H., Chung, H.Y., Kim, N.D., 2013. A novel resveratrol analogue, HS-1793, inhibits hypoxia-induced HIF-1alpha and VEGF expression, and migration in human prostate cancer cells. Int. J. Oncol. 43, 1915–1924.
Li, X., He, S., Li, R., Zhou, X., Zhang, S., Yu, M., Ye, Y., Wang, Y., Huang, C., Wu, M., 2016. Pseudomonas aeruginosa infection augments inflammation through miR-301b repression of c-Myb-mediated immune activation and infiltration. Nat. Microbiol. 1, 16132.
Luan, W., Qian, Y., Ni, X., Bu, X., Xia, Y., Wang, J., Ruan, H., Ma, S., Xu, B., 2017. miR-204-5p acts as a tumor suppressor by targeting matrix metalloproteinases-9 and B-cell lymphoma-2 in malignant melanoma. OncoTarget Ther. 10, 1237–1246.
Ma, Y., Yang, H.Z., Dong, B.J., Zou, H.B., Zhou, Y., Kong, X.M., Huang, Y.R., 2014. Biphasic regulation of autophagy by miR-96 in prostate cancer cells under hypoxia. Oncotarget 5, 9169–9182.
Moroz, A., Delella, F.K., Almeida, R., Lacorte, L.M., Favaro, W.J., Deffune, E., Felisbino, S.L., 2013. Finasteride inhibits human prostate cancer cell invasion through MMP2 and MMP9 downregulation. PLoS One 8, e84757.
Nam, R.K., Benatar, T., Wallis, C.J., Amemiya, Y., Yang, W., Garbens, A., Naeim, M., Sherman, C., Sugar, L., Seth, A., 2016. MiR-301a regulates E-cadherin expression and is predictive of prostate cancer recurrence. Prostate 76, 869–884.
Ni, S., Hu, J., Duan, Y., Shi, S., Li, R., Wu, H., Qu, Y., Li, Y., 2013. Down expression of LRP1B promotes cell migration via RhoA/Cdc42 pathway and actin cytoskeleton remodeling in renal cell cancer. Cancer Sci. 104, 817–825.
Prazeres, H., Torres, J., Rodrigues, F., Pinto, M., Pastoriza, M.C., Gomes, D., Cameselle-Teijeiro, J., Vidal, A., Martins, T.C., Sobrinho-Simoes, M., Soares, P., 2011. Chromosomal, epigenetic and microRNA-mediated inactivation of LRP1B, a modulator of the extracellular environment of thyroid cancer cells. Oncogene 30, 1302–1317.
Taylor, B.S., Schultz, N., Hieronymus, H., Gopalan, A., Xiao, Y., Carver, B.S., Arora, V.K., Kaushik, P., Cerami, E., Reva, B., Antipin, Y., Mitsiades, N., Landers, T., Dolgalev, I., Major, J.E., Wilson, M., Socci, N.D., Lash, A.E., Heguy, A., Eastham, J.A., Scher, H.I., Reuter, V.E., Scardino, P.T., Sander, C., Sawyers, C.L., Gerald, W.L., 2010. Integrative genomic profiling of human prostate cancer. Cancer Cell 18, 11–22.
von Eyben, F.E., Roviello, G., Kiljunen, T., Uprimny, C., Virgolini, I., Kairemo, K., Joensuu, T., 2018. Third-line treatment and (177)Lu-PSMA radioligand therapy of metastatic castration-resistant prostate cancer: a systematic review. Eur. J. Nucl. Med. Mol. Imaging 45, 496–508.
Wang, W., Liu, M., Guan, Y., Wu, Q., 2016a. Hypoxia-responsive Mir-301a and Mir-301b promote radioresistance of prostate cancer cells via downregulating NDRG2. Med. Sci. Monit. 22, 2126–2132.
Wang, K.S., Ma, J., Mi, C., Li, J., Lee, J.J., Jin, X., 2016b. Kamebakaurin inhibits the expression of hypoxia-inducible factor-1alpha and its target genes to confer anti-tumor activity. Oncol. Rep. 35, 2045–2052.
Wang, Z., Sun, P., Gao, C., Chen, J., Li, J., Chen, Z., Xu, M., Shao, J., Zhang, Y., Xie, J., 2017. Down-regulation of LRP1B in colon cancer promoted the growth and migration of cancer cells. Exp. Cell Res. 357, 1–8.
Wu, D., Chen, B., Cui, F., He, X., Wang, W., Wang, M., 2016. Hypoxia-induced microRNA-301b regulates apoptosis by targeting Bim in lung cancer. Cell Prolif. 49, 476–483.
Xiang, S., Chen, H., Luo, X., An, B., Wu, W., Cao, S., Ruan, S., Wang, Z., Weng, L., Zhu, H., Liu, Q., 2018. Isoliquiritigenin suppresses human melanoma growth by targeting miR-301b/LRIG1 signaling. J. Exp. Clin. Cancer Res. 37, 184.
Yan, L., Wang, Y., Liang, J., Liu, Z., Sun, X., Cai, K., 2017. MiR-301b promotes the proliferation, mobility, and epithelial-to-mesenchymal transition of bladder cancer cells by targeting EGR1. Biochemistry and cell biology 95, 571–577.
Yuile, P.G., Tran, M.H., 2002. Survival with brain metastases following radiation therapy. Australas. Radiol. 46, 390–395.
Zhang, C., Lu, J., Liu, B., Cui, Q., Wang, Y., 2016. Primate-specific miR-603 is implicated in the risk and pathogenesis of Alzheimer's disease. Aging. 8, 272–290.